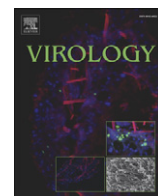


Contents lists available at [SciVerse ScienceDirect](http://SciVerse.Sciencedirect.com)

Virology

journal homepage: www.elsevier.com/locate/yviro

The high risk HPV16 L2 minor capsid protein has multiple transport signals that mediate its nucleocytoplasmic traffic

Shahan Mamoor^a, Zeynep Onder^a, Balasubramanyam Karanam^b, Kihyuck Kwak^b, Jennifer Bordeaux^a, Lauren Crosby^a, Richard B.S. Roden^b, Junona Moroianu^{a,*}

^a Biology Department, Boston College, Chestnut Hill, MA 02467, USA

^b Department of Pathology, The Johns Hopkins University, Baltimore, MD 21231, USA

ARTICLE INFO

Article history:

Received 8 September 2011

Returned to author for revision

10 October 2011

Accepted 4 November 2011

Available online 6 December 2011

Keywords:

Human papillomavirus

L2 minor capsid protein

Nuclear localization signal

Nuclear retention sequence

Nuclear export signal

ABSTRACT

In this study we examined the transport signals contributing to HPV16 L2 nucleocytoplasmic traffic using confocal microscopy analysis of enhanced green fluorescent protein–L2 (EGFP–L2) fusions expressed in HeLa cells. We confirmed that both nuclear localization signals (NLSs), the nNLS (1MRHKRSKRTRK12) and cNLS (456RKRKR461), previously characterized *in vitro* (Darshan et al., 2004), function independently *in vivo*. We discovered that a middle region rich in arginine residues (296SRRTGIRYSRIGNKQTLRTRS316) functions as a nuclear retention sequence (NRS), as mutagenesis of critical arginine residues within this NRS reduced the fraction of L2 in the nucleus despite the presence of both NLSs. Significantly, the infectivity of HPV16 pseudoviruses containing either RR297AA or RR297EE within the L2 NRS was strongly reduced both in HaCaT cells and in a murine challenge model. Experiments using Ratjadone A nuclear export inhibitor and mutation-localization analysis lead to the discovery of a leucine-rich nuclear export signal (₄₆₂LPYFFSDVSL) mediating 16L2 nuclear export. These data indicate that HPV16 L2 nucleocytoplasmic traffic is dependent on multiple functional transport signals.

© 2011 Elsevier Inc. All rights reserved.

Introduction

Human papillomavirus (HPV) infection is associated with more than 99% of cervical cancers, and approximately 500,000 new cases of cervical cancer are diagnosed each year with the mean age for development of malignancy being 52 years. In addition, a high percent of anal, perianal, vulvar, penile, oropharyngeal and non-melanoma skin cancers are linked to HPV infections. Some 30 distinct HPV genotypes are preferentially infecting anogenital mucosal epithelial tissues. Mucosal HPVs have demonstrated varying degrees of oncogenic potential, with some classified as high risk, such as types 16, 18, 31 and 45, and others as low risk, such as types 6 and 11. High risk HPVs are frequently detected in invasive cervical carcinomas, whereas the low risk types are more often associated with benign exophytic condylomas (Longworth and Laimins, 2004; zur Hausen, 2009).

HPVs are small, non-enveloped, icosahedral DNA viruses (55–60 nm in diameter) consisting of a single molecule of 8 kb double-stranded circular DNA contained within a icosahedral capsid

composed of 72L1 homopentamers (capsomers). The L2 minor capsid protein is present in up to 72 copies per virion, most likely one L2 molecule in the center of each L1 capsomer (Buck et al., 2008). Although several aspects of the viral life cycle can occur in organotypic raft culture in the absence of L2 protein, virion progeny encapsidated 10-fold less viral DNA and there was an over 100-fold reduction in infectivity. These data suggest that L2 plays additional role(s) in the viral life cycle distinct from genome encapsidation (Holmgren et al., 2005). Indeed there is evidence that L2 may function in endosomal escape of incoming virions (Kamper et al., 2006) and nuclear traffic of the viral genome (Day et al., 2004; Fay et al., 2004; Roden et al., 2001).

L2 protein was found to interact with several host proteins including actin (Yang et al., 2003), the microtubule-binding protein dynein (Florin et al., 2006), and the endoplasmic reticulum t-snare Syntaxin-18 (Laniosz et al., 2007).

Different mechanisms of endocytosis (involving either clathrin, caveolin, or tetraspanin domains) have been proposed for different papillomavirus types (Day et al., 2003; Sapp and Bienkowska-Haba, 2009; Smith et al., 2007, 2008; Spoden et al., 2008). The L2 minor capsid protein enters the nucleus twice during the viral life cycle: in the initial phase of infection when it accompanies the viral genome to the nucleus, and in the productive phase of infection when together with L1 major capsid protein it is involved in encapsidation of the newly replicated viral DNA. Cleavage of L2 at a furin consensus site located in the N-terminus was reported to be

Abbreviations: HPV, human papillomavirus; NLS, nuclear localization signal; NES, nuclear export signal; NRS, nuclear retention sequence; EGFP, enhanced green fluorescent protein.

* Corresponding author at: Boston College, Biology Department, Higgins Hall, room 578, 140 Commonwealth Avenue, Chestnut Hill, MA 02467, USA. Fax: +1 617 552 2011.

E-mail address: moroianu@bc.edu (J. Moroianu).

required during the initial stage of infection, although it is not known what percent of the L2 molecules are processed by furin (Richards et al., 2006). Recently, it has been shown that papillomavirus infection also requires γ -secretase at a step after disassembly of the virions in endosomes and before the entry of the L2-viral genome complex into the nucleus (Karanam et al., 2010). The target for the γ -secretase cleavage remains to be determined, and potential candidates are either the L2 itself or an intracellular receptor (Karanam et al., 2010). During the productive phase of infection the expression and nuclear import of L2 in natural lesions precede expression and nuclear translocation of L1 major capsid protein (Florin et al., 2002). The L2 protein has a diffuse nuclear localization in cervical intraepithelial neoplasia lesions and HPV16-transduced organotypic cultures (Lin et al., 2009). We have previously determined that HPV16 L2 contains two nuclear localization signals (NLSs), one at the amino-terminus (nNLS) and the other at the carboxy-terminus (cNLS). Either NLS could mediate nuclear import of a GST reporter in the *in vitro* nuclear import assays in digitonin-permeabilized HeLa cells via interaction with specific karyopherins (Darshan et al., 2004). We established that HPV16 L2 can interact with Kap α 2 β 1 heterodimers, Kap β 2 and Kap β 3 nuclear import receptors via its NLSs and enter the nucleus via multiple pathways (Darshan et al., 2004). However, the transport signals contributing to the nucleocytoplasmic traffic of HPV16 L2 *in vivo* have not been examined. In this study we performed a detailed *in vivo* analysis of the nucleocytoplasmic transport signals of HPV16 L2 capsid protein using fluorescent confocal microscopy analysis of different EGFP–16L2 fusions expressed in HeLa cells. We confirmed that the two NLSs previously characterized *in vitro* can function independently *in vivo* mediating the nuclear localization of HPV16 L2 protein. Moreover, we discovered that HPV16 L2 has an arginine-rich nuclear retention signal (NRS) mediating its nuclear retention and accumulation, and also a leucine-rich nuclear export signal (NES) mediating its nuclear export in a CRM1-dependent manner. Significantly, mutations of critical residues in the NRS strongly reduced HPV16 infectivity in a murine challenge model and in HaCaT cells. These data indicate that the nucleocytoplasmic traffic of HPV16 L2 is more complex than previously anticipated and it is mediated by multiple transport signals.

Results

Both the nNLS and cNLS of HPV16 L2 protein can function independently in vivo

Previously we have established that the high risk HPV16 L2 minor capsid protein has two NLSs that can interact with karyopherins/importins and mediate the nuclear import of 16L2 in digitonin-permeabilized HeLa cells *in vitro* (Darshan et al., 2004).

To investigate the localization of HPV16 L2 in HeLa cells we transiently transfected HeLa cells with an EGFP–16L2 fusion plasmid (EGFP fused at the N-terminus of 16L2) and analyzed the localization of the translated EGFP–16L2. The transfected HeLa cells were immunostained with the RG-1 mouse anti-L2 monoclonal antibody, followed by a secondary anti-mouse IgG conjugated to Alexa Fluor 594. Analysis of both the EGFP fluorescence and the 16L2 immunostaining using confocal fluorescence microscopy revealed that the EGFP–16L2 is nuclear in the majority of the cells (Figs. 1A and B). In order to analyze the roles of the nNLS and cNLS *in vivo* we generated the following plasmid mutants: EGFP–16L2 Δ N lacking the nNLS, EGFP–16L2 Δ C lacking the cNLS and the EGFP–16L2 Δ N Δ C lacking both NLSs, and transiently transfected HeLa cells with these mutant plasmids. Both the EGFP–16L2 Δ N and the EGFP–16L2 Δ C were localized in the nucleus in the majority of cells like the EGFP–16L2 wild type, whereas the EGFP–16L2 Δ N Δ C double mutant had a cytoplasmic and pancellular localization (Figs. 1A and B). These data

suggest that both the nNLS and the cNLS can independently mediate the nuclear localization of 16L2 minor capsid protein *in vivo*.

HPV16 L2 has a nuclear retention sequence rich in arginine residues

HPV16 L2 has a middle region rich in arginine residues (₂₉₆SRRTGIRYSRIGNKQTLRTRS₃₁₆), which cannot mediate nuclear import of a GST reporter in digitonin-permeabilized HeLa cells (Darshan et al., 2004). To investigate if this arginine-rich region has any role in the nuclear localization of 16L2 we generated several mutants: EGFP–16L2ms1 (RR297EE), EGFP–16L2ms2 (RTR₃₁₃EEE), and EGFP–16L2ms3 (ms1 and ms2). These mutants retain both the cNLS and nNLS, and contain glutamic acid substitutions in the arginine-rich middle region. Confocal microscopy analysis of the localization of these L2 middle region mutants in HeLa cells revealed that mutation of either Arg pair affects the retention of EGFP–16L2 in the nucleus (Fig. 2). Quantitative analysis revealed a mixed phenotype, with either ms1 or ms2 mutation reducing the percent of cells with mostly nuclear localization to ~30%, and the rest of the cells having pancellular or mostly cytoplasmic localization for EGFP–16L2ms1 and EGFP–16L2ms2 (Fig. 3). The double mutant EGFP–16L2ms3 showed a similar reduction in nuclear localization and increase in pancellular and mostly cytoplasmic localization, with no increase in the severity of the nuclear retention defect in comparison with the ms1 and ms2 mutants (Fig. 3). Together, the data from these experiments indicate that this arginine-rich sequence in the middle region of HPV16 L2 functions as a nuclear retention sequence (NRS) *in vivo* and the Arg residues are critical for this function. Furthermore, the cytoplasmic and pancellular localization of 16L2 nuclear retention mutants containing both NLSs suggests an active export mechanism for 16L2, as EGFP–16L2 is well above the limit for passive diffusion into the cytoplasm. Note that there is a larger variation between different experiments for the L2 nuclear retention mutants regarding their percent of cells with pancellular and cytoplasmic localization, further suggesting that they shuttle between the nucleus and the cytoplasm. The same ms1, ms2 and ms3 mutations in the context of EGFP–16L2 Δ N Δ C, lacking both NLSs, completely changed the pancellular localization that was still present in some 50% of cells to cytoplasm (Fig. 1B and Fig. S1, A and B). This suggests that the 16L2 NRS may have some very weak nuclear import activity.

HPV16 L2 protein can be exported out of the nucleus in a CRM1-dependent manner

The fact that EGFP–16L2 nuclear retention mutants displayed a mixed phenotype, with a majority of cells containing pancellular and mostly cytoplasmic localization, suggested that these 16L2 nuclear retention mutants were being exported from the nucleus into the cytoplasm via a signal-mediated pathway. A major nuclear export pathway is mediated by the CRM1 nuclear export receptor, which mediates nuclear export of cargoes containing leucine-rich NESs. To analyze if the CRM1 pathway is involved in the nuclear export of 16L2 nuclear retention mutants we used a specific chemical inhibitor of CRM1, ratjadone A (RJA). RJA inhibition functions similarly to Leptomycin B (LMB) inhibition, it covalently modifies a cysteine residue in the NES-binding pocket of CRM1 resulting in inhibition of NES-binding (Hutten and Kehlenbach, 2007; Meissner et al., 2004). Twenty-one hours after transfection of HeLa cells with EGFP–16L2ms1, EGFP–16L2ms2, or EGFP–16L2ms3, the cells were treated with 10 ng/mL RJA for three and a half hours. After the RJA treatment, the cells were fixed, immunostained and analyzed by confocal fluorescence microscopy. As positive and negative controls for the RJA drug treatment, we used the EGFP–16E7–NES_{rev} plasmid that contains the HPV16 E7 oncoprotein fused to the strong leucine-rich NES of HIV-1 Rev, or EGFP alone,

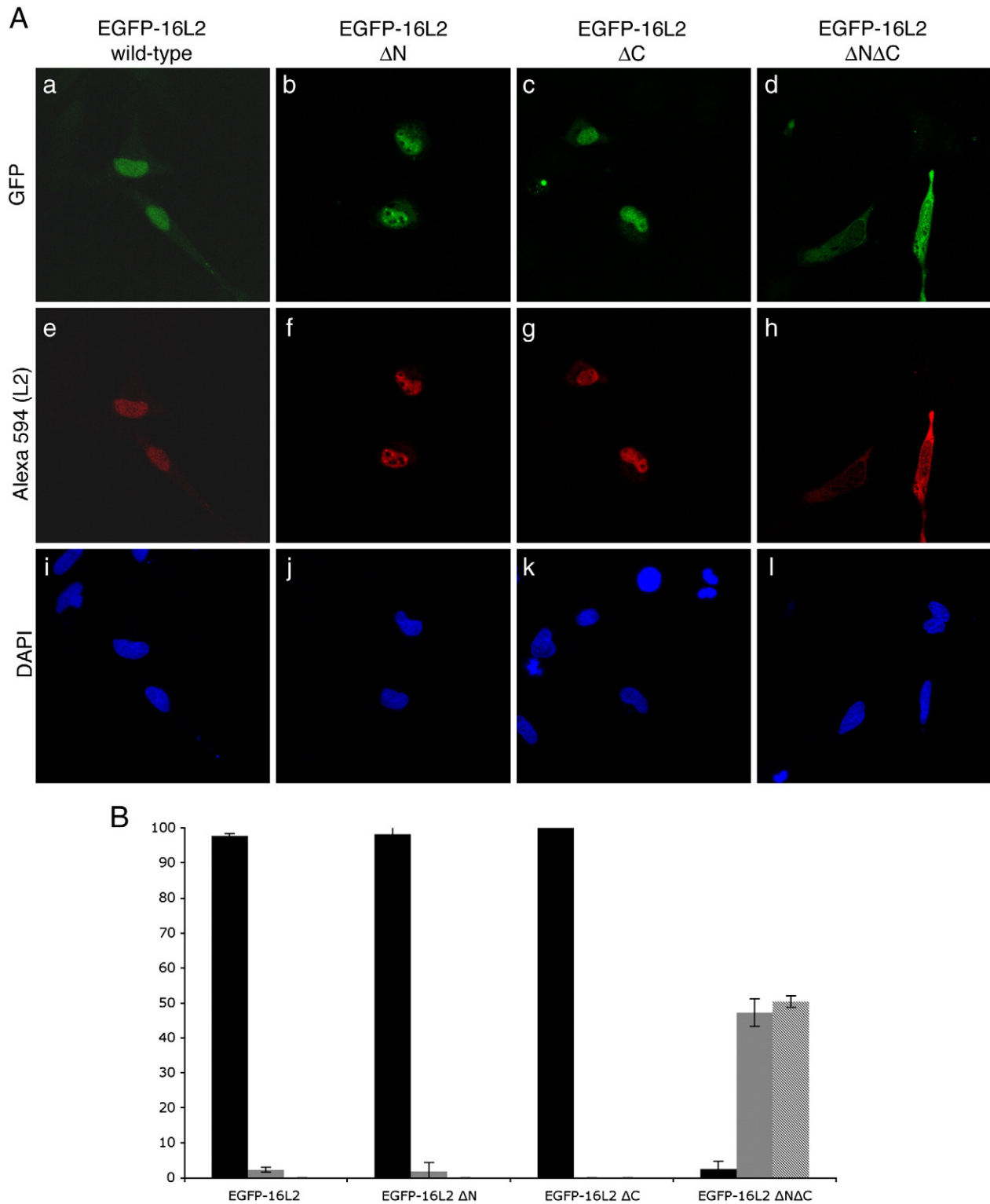


Fig. 1. EGFP-16L2 is localized in the nucleus, and both the nNLS and cNLS of 16L2 can function independently *in vivo*. A. HeLa cells were fixed 24 h after transfection with either EGFP-16L2 (subpanels a, e and i), EGFP-16L2 Δ N (subpanels b, f, and j), EGFP-16L2 Δ C (subpanels c, g, and k), or EGFP-16L2 Δ N Δ C (subpanels d, h, and l), immunostained with RG-1 monoclonal antibody against L2 (and a corresponding IgG conjugated to Alexa 594), and examined by confocal laser-scanning microscopy. Anti-L2 staining is shown in the middle row (subpanels e, f, g, and h respectively), while DAPI (4', 6'-diamidino-2-phenylindole) staining of the nuclei is shown in the bottom row (subpanels i, j, k and l, respectively). B. Cells were phenotyped as having either mostly nuclear (black bars), pan-cellular (gray bars), or mostly cytoplasmic localization (striped bars) of EGFP-16L2 or EGFP-16L2 mutants, and quantitative analysis is represented graphically with average and standard deviation.

respectively. As expected, the localization of the translated EGFP-16E7-NES_{rev} was cytoplasmic in a majority of cells transfected and the RJA treatment resulted in a dramatic re-localization of the EGFP-16E7-NES_{rev} fusion protein into the nucleus in the majority

of cells (data not shown). The pan-cellular localization of EGFP was not affected by the RJA treatment (data not shown). The RJA treatment resulted in a significant re-localization of the 16L2 nuclear retention mutants to the nucleus (Fig. 3). The RJA treatment of

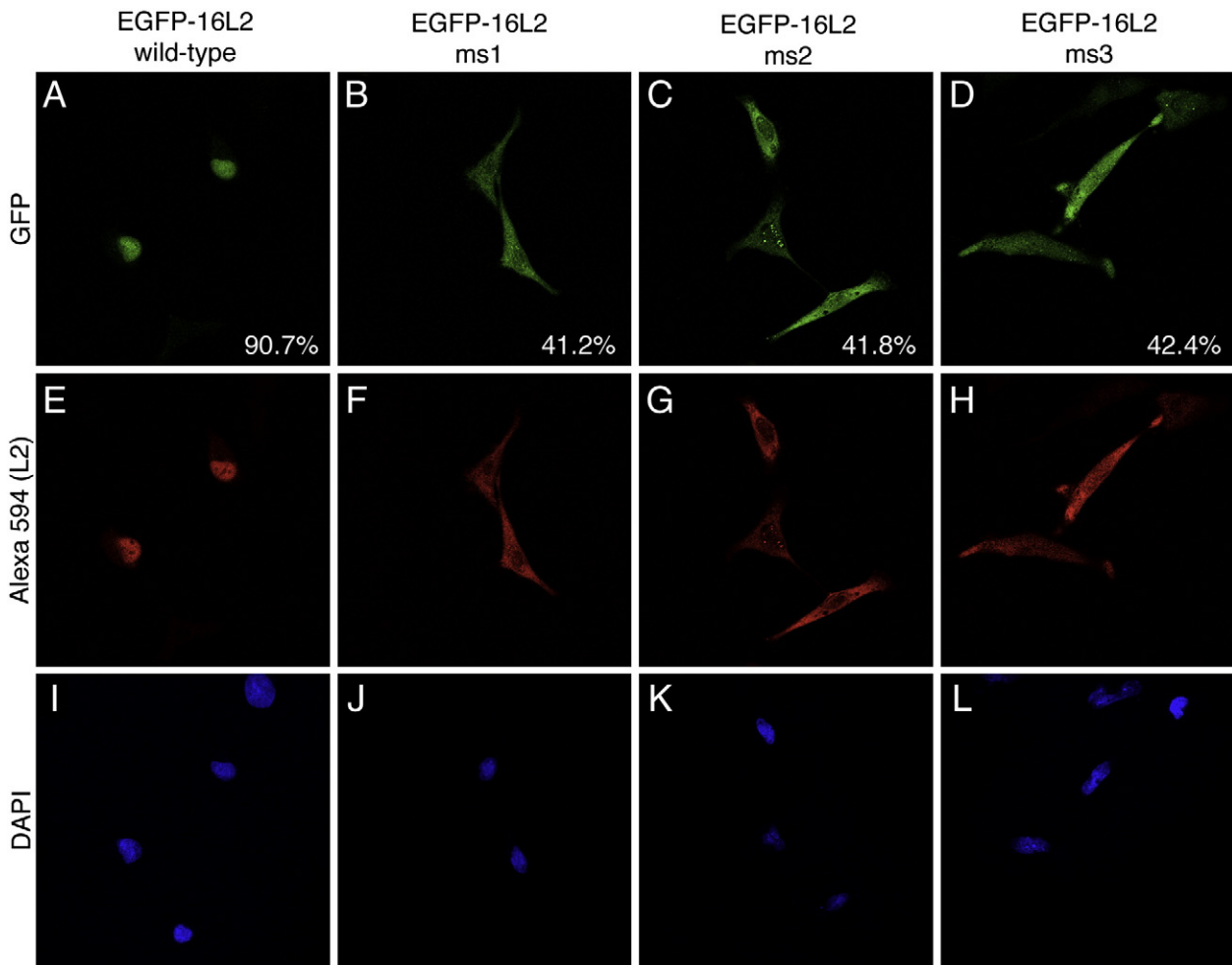


Fig. 2. Mutation of critical arginine residues in a middle sequence to glutamic acid affects the nuclear retention of HPV16 L2, in the presence of both NLSs. HeLa cells were transfected with either EGFP-16L2 (panels A, E, and I), EGFP-16L2ms1 (panels B, F, and J), EGFP-16L2ms2 (panels C, G, and K), or EGFP-16L2ms3 (panels D, H, and L), fixed after 24 h and immunostained with RG-1 monoclonal antibody against L2 (and a corresponding IgG conjugated to Alexa 594), and then examined by confocal laser-scanning microscopy. Anti-L2 staining is shown in the middle row (panels E, F, G, and H, respectively), while DAPI staining of the nuclei is shown in the bottom row (panels I, J, K, and L, respectively). The percent of cells with a specific localization of EGFP-16L2 or mutants is also indicated on the panels.

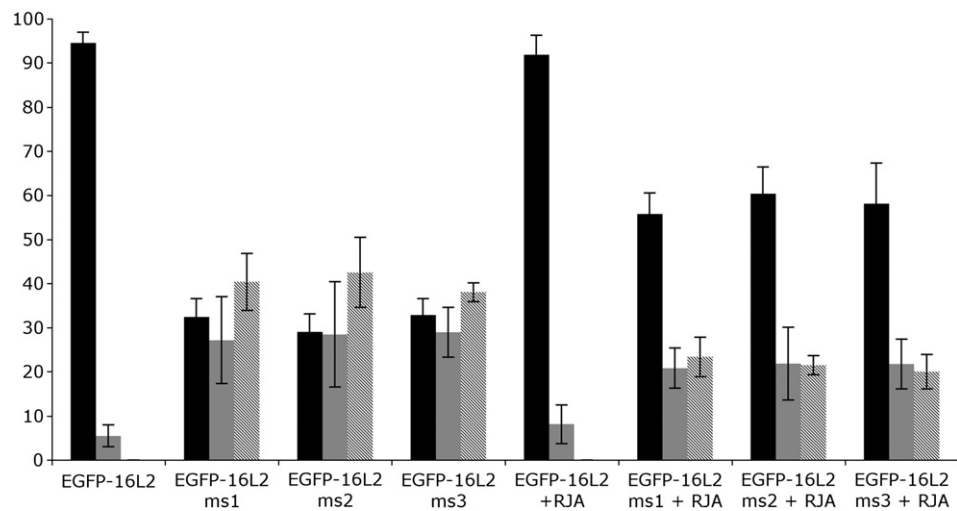


Fig. 3. HPV16 L2 nuclear retention mutants re-localize to the nucleus in the presence of RJA, a specific inhibitor of CRM1 nuclear export receptor. Twenty-one hours post-transfection with either EGFP-L2, EGFP-16L2ms1, EGFP-16L2ms2, or EGFP-16L2ms3, HeLa cells were treated with either fresh DMEM or 10 ng/mL RJA for 3.5 h. After fixation, cells were immunostained with RG-1 monoclonal antibody against L2 (and a corresponding IgG conjugated to Alexa 594) and examined by confocal laser-scanning microscopy. Cells were phenotyped as having either mostly nuclear (black bars), pan-cellular (gray bars), or mostly cytoplasmic (striped bars) localization of EGFP-16L2 or EGFP-16L2 mutants, and quantitative analysis is represented graphically with average and standard deviation.

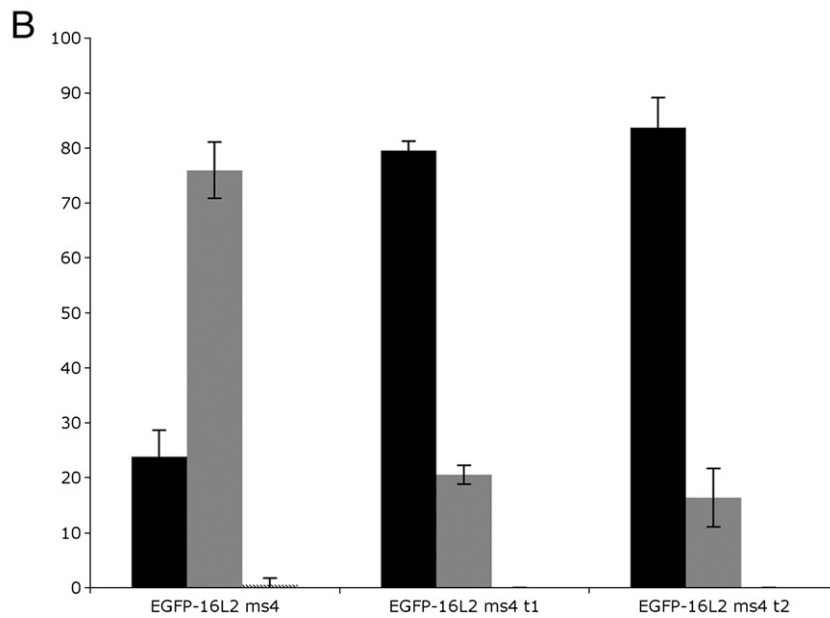
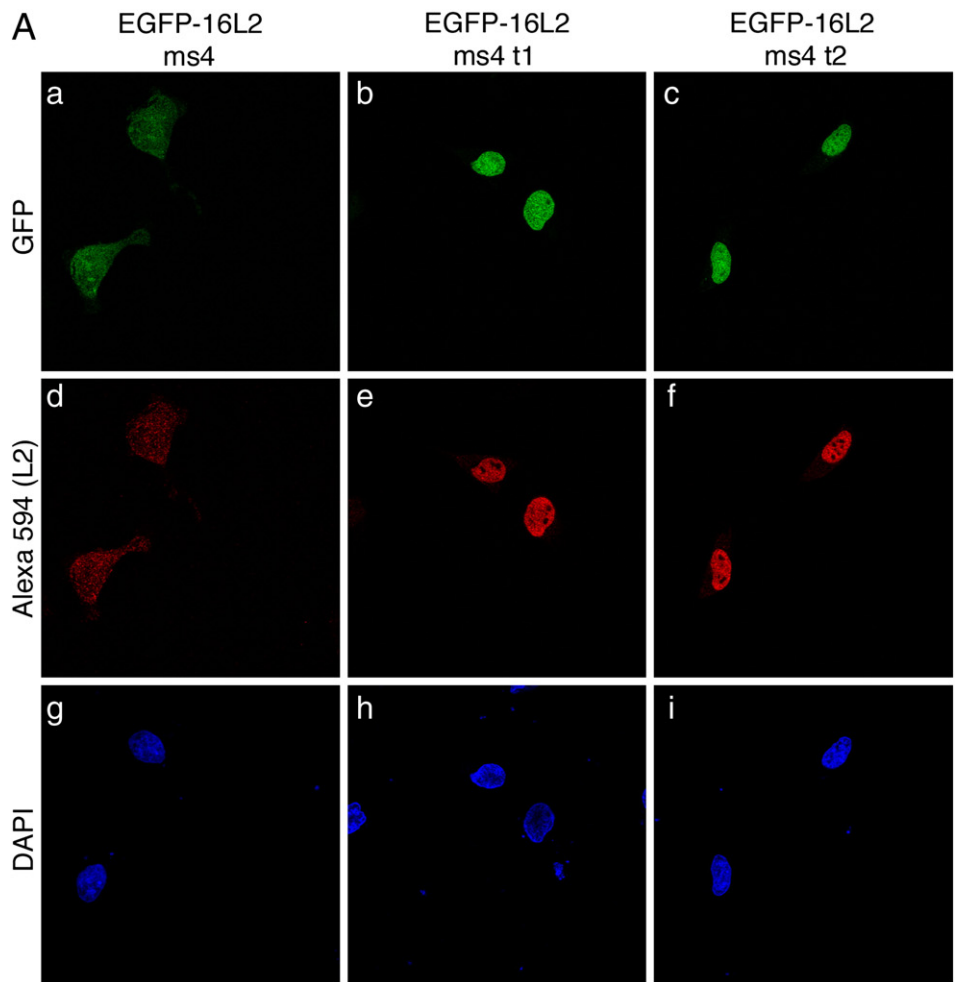


Fig. 4. Deletions in a potential cNES rescue the nuclear localization of the 16L2ms4 nuclear retention mutant. A. HeLa cells were fixed 24 h after transfection with either EGFP-16L2ms4 (subpanels a, d, and g), EGFP-16L2ms4t1 (subpanels b, e, and h) or EGFP-16L2ms4t2 (subpanels c, f, and i), immunostained with RG-1 monoclonal antibody against L2 (and a corresponding IgG conjugated to Alexa 594), and examined by confocal microscopy. Anti-L2 staining is shown in the middle row (subpanels d, e, and f), while DAPI staining of the nuclei is shown in the bottom row (subpanels g, h, and i). B. Cells were phenotyped as having either mostly nuclear (black bars), pancellular (gray bars), or mostly cytoplasmic localization (striped bars), and the quantitative analysis is represented graphically in B.

EGFP-16L2ms1, EGFP-16L2ms2, and EGFP-16L2ms3 led to an increase to ~60% of the transfected cells having mostly nuclear localization and a concomitant decrease to 20% of cells having mostly cytoplasmic localization (Fig. 3). The fact that the RJA treatment induced re-localization of EGFP-16L2 nuclear retention mutants was a strong indication that the 16L2 mutants were shuttling between the nucleus and the cytoplasm. To eliminate the possibility that the mutation (i.e. charge of glutamic acid) was leading to some partial misfolding of the EGFP-16L2 nuclear retention mutants, we also generated the EGFP-16L2ms4 (RR297AA) and EGFP-16L2ms5 (RTR313AAA) mutants. Analysis of their localization revealed a mixed phenotype, with either ms4 and ms5 mutation reducing the percent of cells with mostly nuclear localization to ~25%, and ~50% respectively, with the rest of cells having a pancellular localization (Figs. 4B and 5B).

HPV16 L2 has a leucine-rich NES mediating its nuclear export in a CRM1-dependent manner

The RJA results of partial re-localization of 16L2 nuclear retention mutants suggest that 16L2 shuttles between the nucleus and the cytoplasm, and that 16L2 exits the nucleus via a CRM1-dependent pathway, either directly through its own NES or indirectly through binding to an NES-containing cellular protein. Analysis of the HPV16 L2 sequence revealed the existence of two potential leucine-rich NESs that match the NES consensus motif: one toward the N-terminus (nNES: $_{51}$ MGVFFGGLG $_{60}$) and the other at the C-terminus (cNES: $_{462}$ LPYFFSDVSL $_{471}$), followed by only two alanine residues. To investigate if the potential nNES is functional and can mediate the nuclear export of 16L2 we generated the following nNES mutants in the EGFP-16L2ms4 background: s1 (FF54AA) and s2 (LG158AAA),

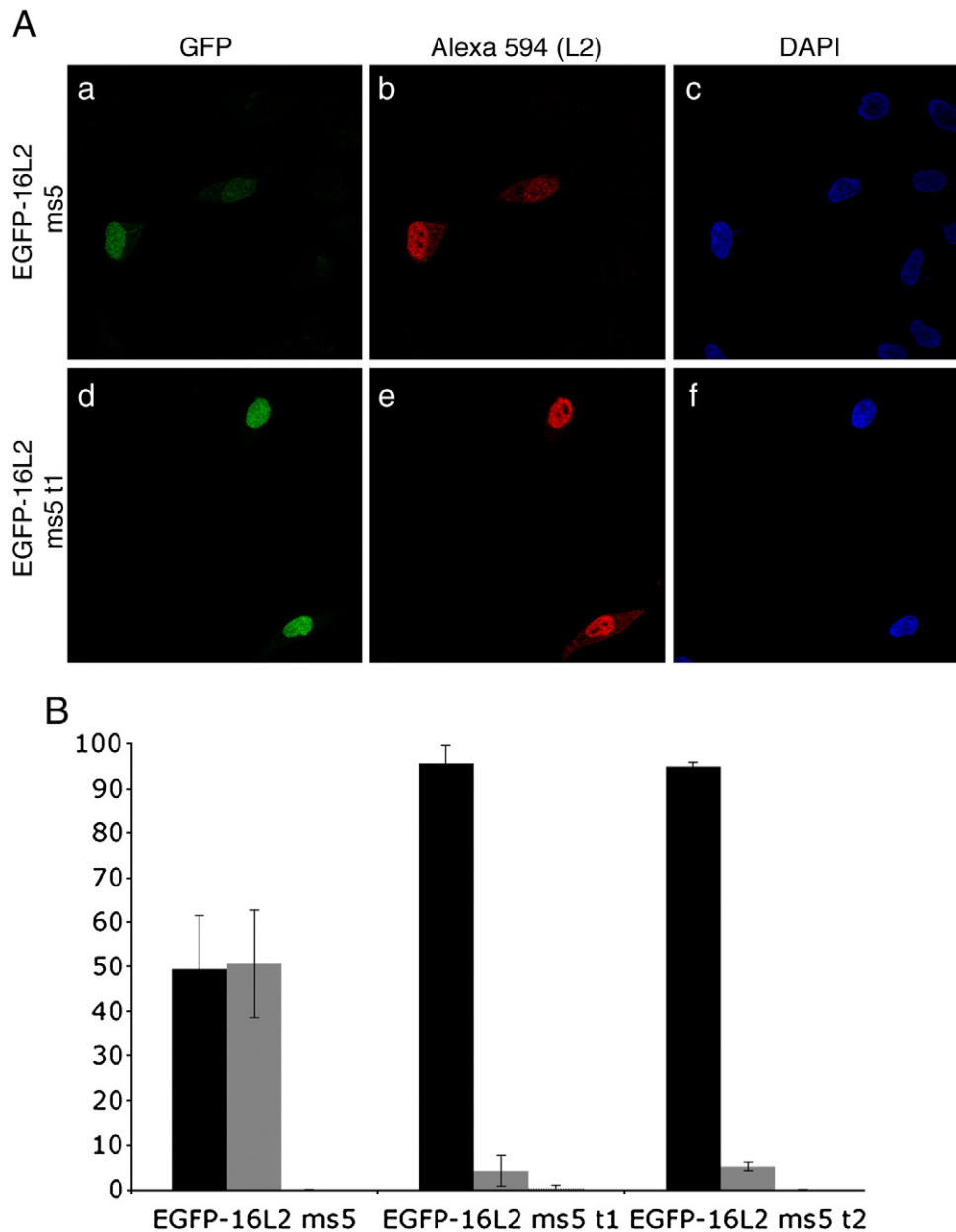


Fig. 5. Deletion of the cNES rescues the nuclear localization of the 16L2ms5 nuclear retention mutant. A. HeLa cells were fixed 24 h after transfection with either EGFP-16L2ms5 (subpanels a, b, and c), EGFP-16L2ms5t1 (subpanels d, e, and f), or EGFP-16L2ms5t2, immunostained with RG-1 monoclonal antibody against L2 (and a corresponding IgG conjugated to Alexa 594), and examined by confocal microscopy. B. Cells were phenotyped as having either mostly nuclear (black bars), pancellular (gray bars), or mostly cytoplasmic localization (striped bars), and the quantitative analysis is represented graphically with average and standard deviation.

and performed transfections of HeLa cells with the EGFP–16L2ms4, EGFP–16L2ms4s1 and 16L2ms4s2 mutant plasmids. Analysis of the localization of these translated EGFP–16L2 mutants revealed similar pancellular localizations for the EGFP–16L2ms4, EGFP–16L2ms4s1 and EGFP–16L2ms4s2 proteins in the majority of cells (Fig. S2, A and B). These data suggest that this potential nNES is not a functional NES involved in nuclear export of 16L2 minor capsid protein. This is not surprising as this sequence is located in a highly hydrophobic region of 16L2, which could be buried inside the molecule and not exposed at the surface.

To investigate if the potential cNES (₄₆₂LPYFFSDVSL₄₇₁) functions in nuclear export of 16L2 protein we generated the following two cNES truncated mutants in the EGFP–16L2ms4 nuclear retention mutant background: t1: ₄₆₂L_ (containing a stop codon at ₄₆₃P), and t2: ₄₆₂LPYFFSD_ (containing a stop codon at ₄₆₉V). After transient transfection of HeLa cells with these plasmids we examined the localization of the expressed EGFP–16L2ms4, EGFP–16L2ms4t1, and EGFP–16L2ms4t2 mutants using fluorescence confocal microscopy. Interestingly, both the t1 and t2 cNES deletion mutants had a mostly nuclear localization in the majority of cells in contrast with the pancellular localization of EGFP–16L2ms4 (Figs. 4A and B). These data indicate that the t1 and t2 deletions in the cNES block nuclear export and cause accumulation of the EGFP–16L2ms4 nuclear retention mutant in the nucleus. Overall the data suggest that the cNES (₄₆₂LPYFFSDVSL₄₇₁) functions in nuclear export of 16L2 minor capsid protein and that the ₄₆₉V and ₄₇₁L are essential amino acids for the cNES export function.

We also generated t1 and t2 deletions in the 16L2ms5 nuclear retention mutant and analyzed their localization in HeLa cells in comparison with the EGFP–16L2ms5. The EGFP–16L2ms5 had a mostly nuclear localization in some 50% of cells and a pancellular localization in the rest of the transfected cells (Figs. 5A and B). In contrast, the EGFP–16L2ms5t1 and EGFP–16L2ms5t2 had a nuclear localization in over 90% of cells (Figs. 5A and B). We obtained a similar rescue of the nuclear localization to over 90% of transfected cells for the EGFP–16L2ms3t1 mutant (Fig. S3). Overall, these data indicate that deletions in the cNES rescue the nuclear localization of the 16L2ms5 and 16L2ms3 nuclear retention mutants, further suggesting that this cNES functions in nuclear export of 16L2.

We next examined the roles of ₄₆₂L, ₄₆₅FF amino acids in the nuclear export function of 16L2's cNES by analyzing the localization of EGFP–16L2ms4 L462A and EGFP–16L2ms4 FF465AA mutants in comparison with EGFP–16L2ms4 after transfection in HeLa cells. Both the L462A and FF465AA mutations rescued the nuclear localization of the EGFP–16L2ms4 nuclear retention mutant to over 90% of transfected cells (Figs. 6A and B). These data confirm that the cNES functions in nuclear export of 16L2 and that the ₄₆₂L, ₄₆₅FF amino acids play a critical role in the export function.

A scheme of all the nucleocytoplasmic transport signals of HPV16 L2 minor capsid protein, the nNLS, cNLS, the NRS in the middle of the protein and the cNES located at the C-terminus of L2, is shown in Fig. 7.

Pseudovirions containing the 16L2 NRS mutants, RR297EE and RR297AA, showed strongly reduced infectivity upon murine vaginal challenge and in HaCaT cells

To investigate if the NRS and/or the NES play a role during the HPV16 infection we generated HPV16 pseudoviruses containing either wild type HPV16 L2, or L2 with mutations targeting either the NRS or NES. Incorporation of these mutations targeting either the NRS or NES did not adversely impact the yield of pseudovirus in the peak fraction from the Optiprep gradient or the co-assembly of L1 with L2 as demonstrated by the L2 immunoblot of wild type and mutant pseudoviruses (Fig. S4), and had limited effect upon the presence

of Benzonase-resistant luciferase reporter DNA as determined by Q-PCR (Table 1). This suggests that neither the NRS nor the NES are critical for the assembly of the capsid and encapsidation of DNA and that these minimal mutations do not cause structural defects in the capsid. Therefore we sought to determine their role in the early events of infection by examining the infectivity of each pseudovirion preparation by vaginal challenge of mice as previously described (Roberts et al., 2007). As negative control we used mice with passively transferred HPV16 L1 VLP anti-serum 1 day prior to vaginal challenge. For both NRS L2 mutants, RR297AA and RR297EE, the infectivity was strongly reduced almost to the background level of the negative control (Fig. 8). Since this effect cannot be accounted for by reduced pseudovirion assembly and L2 incorporation, these data clearly suggest that the nuclear retention of HPV16 L2 mediated by its NRS is important during the initial phase of viral infection. For the NES L2 mutant FF465AA defective in nuclear export, the infectivity was significantly reduced to some 13% of the wild type (Fig. 8). Although less pronounced, there was a reduction in infectivity for the NES L2 deletion mutant V469_ to 42% of the wild type average level (Fig. 8).

We also performed infectivity assays in HaCaT cells with HPV16 L2 wild type and mutant pseudoviruses in the absence or presence of the neutralizing RG1 antibody. The neutralization with the RG1 antibody was used as a negative control. For both NRS L2 mutants, RR297AA and RR297EE, the infectivity in HaCaT keratinocytes was strongly reduced to background levels of the negative control with the neutralizing RG1 antibody (Fig. 9). These data correlate with the *in vivo* infectivity results in the mouse vaginal model, further supporting that the nuclear retention of HPV16 L2 mediated by its NRS is critical during the initial phase of viral infection. There was also a reduction in infectivity in HaCaT cells with the two NES L2 mutants, FF465AA and V469_, although less pronounced (Fig. 9), similarly with the results obtained in the murine vaginal challenge model.

Discussion

Nuclear localization of L2 minor capsid protein is required for viral genome localization to the nucleus during the initial phase of infection, and for genome encapsidation and assembly of infectious viral progeny during the productive phase of infection (Day et al., 2004; Fay et al., 2004; Florin et al., 2002; Holmgren et al., 2005).

In this study, we investigated the signals that dictate the nucleocytoplasmic transport of the HPV16 L2 minor capsid protein in living HeLa cells using confocal microscopy analysis of the localization of different expressed EGFP–16L2 mutants. Data from transient transfections with EGFP–16L2 wild type and EGFP–16L2ΔN, ΔC, ΔNΔC deletion mutants indicated that both the cNLS and nNLS of 16L2 could independently mediate the nuclear localization of 16L2 *in vivo*. This is consistent with our previous biochemical data demonstrating that 16L2 has an nNLS and a cNLS, and either NLS can mediate nuclear import of 16L2 *in vitro* in digitonin-permeabilized HeLa cells via interactions with specific karyopherins (Darshan et al., 2004). The mostly cytoplasmic localization in some 50% cells and pancellular localization in the remaining 50% cells of the EGFP–16L2ΔNΔC lacking both NLSs suggested that there is no additional strong NLS in the 16L2. This is in agreement with our previous findings that showed that recombinant 16L2ΔNΔC could not be imported into the nuclei of digitonin-permeabilized HeLa cells, and that a middle arginine-rich region could not mediate nuclear import of a GST reporter *in vitro* (Darshan et al., 2004). We have previously shown that the high risk HPV18 L2 and the low risk HPV11 L2 have two similar NLSs (Table 2), and that both the nNLS and the cNLS can function independently *in vivo* in mediating the nuclear localization of these L2 proteins via interactions with specific karyopherins (Bordeaux et al., 2006; Klucsevsek et al., 2006). Also, the low risk HPV6b L2 has both an nNLS and a cNLS (Table 2), which can mediate the nuclear localization of HPV6b L2 *in vivo* (Sun et al., 1995). Interestingly, BPV1 L2 has

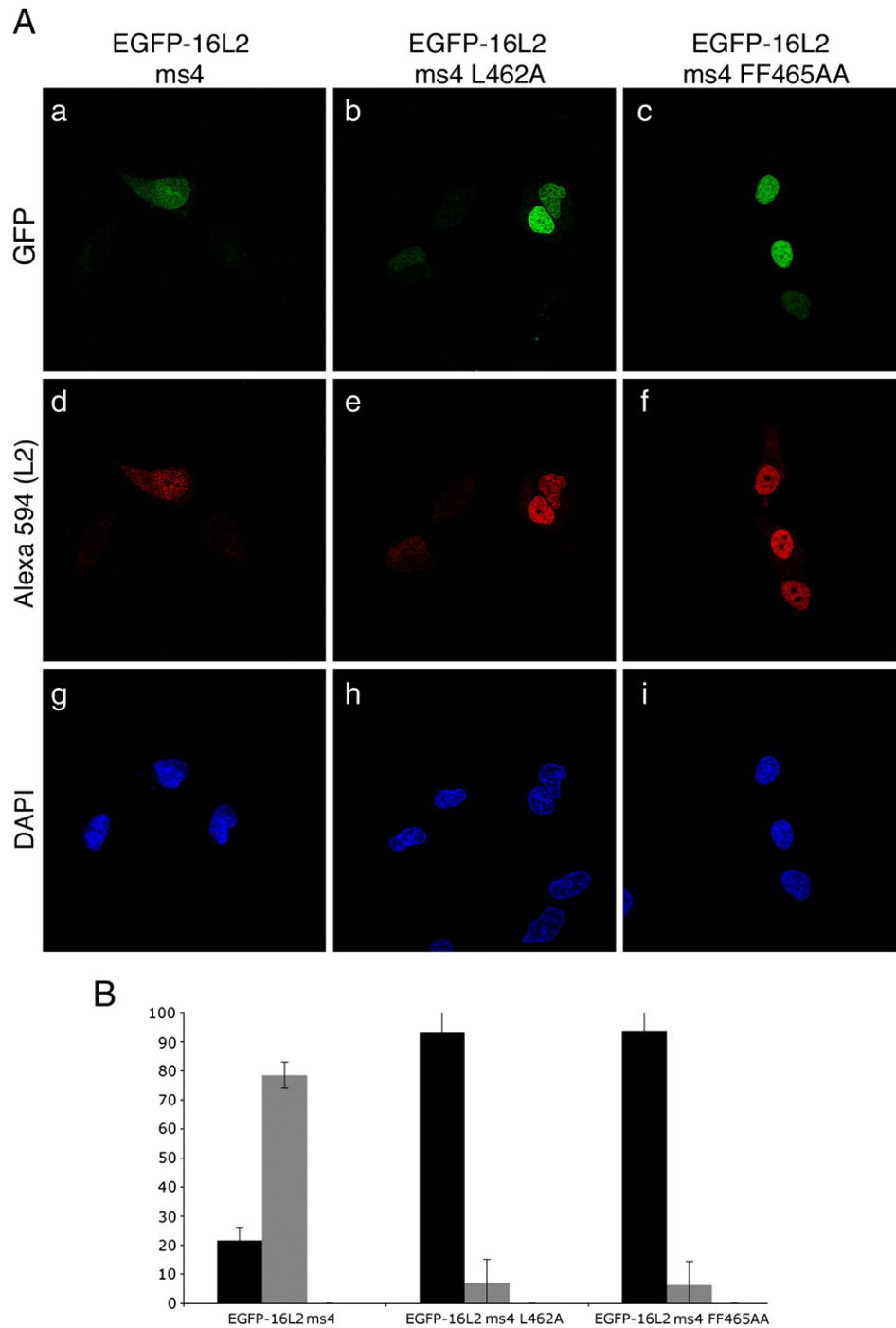


Fig. 6. The effect of L462A and FF465AA mutations in the cNES on the localization of the 16L2ms4 nuclear retention mutant. HeLa cells were fixed 24 h after transfection with either EGFP-16L2ms4 (subpanels A, D, and G), EGFP-16L2ms4 L462A (subpanels b, e, and h) or EGFP-16L2ms4 FF465AA (subpanels c, f, and i), immunostained with RG-1 monoclonal antibody against L2 (and a corresponding IgG conjugated to Alexa 594), and examined by confocal microscopy. Anti-L2 staining is shown in the middle row (subpanels d, e, and f), while DAPI staining of the nuclei is shown in the bottom row (subpanels g, h, and i). B. Cells were phenotyped as having either mostly nuclear (black bars), pancellular (gray bars), or mostly cytoplasmic localization (striped bars), and the quantitative analysis is represented graphically with average and standard deviation.

two similar NLSs and deletion of either the nNLS or the cNLS inhibits infectivity at a step after cell entry of BPV1 pseudovirions (Fay et al., 2004; Roden et al., 2001).

Mutation of the arginine pairs 297RR and 313 RTR to either glutamic acid or alanine affected the nuclear retention of 16L2 in the presence of both of its NLSs suggesting that this middle arginine-rich sequence functions in the nuclear retention of 16L2 *in vivo* and that these arginine residues are essential for the NRS function. A previous study had suggested a possible role for this region in the nuclear

retention of low risk HPV6b L2 minor capsid protein (Sun et al., 1995). Significantly, the 16L2's NRS is well conserved in other HPV L2 proteins, including the high risk HPV types 18, 31 and 33 and the low risk HPV types 6 and 11 (Table 3). It will be of interest to see if the corresponding NRS sequence has a similar function in these L2 proteins of other HPV types. At this point we can only speculate on the molecular mechanism(s) by which the NRS mediates retention of 16L2 in the nucleus. The 16L2 protein could form a complex with a nuclear protein(s) or could interact with the negatively charged

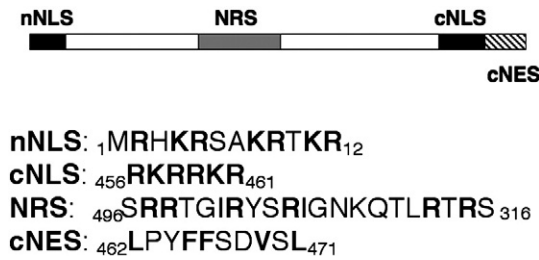


Fig. 7. A scheme of the nucleocytoplasmic transport signals of HPV16 L2 minor capsid protein.

phosphate groups of the DNA backbone via the positively charged arginine residues. Although we have previously shown that the NRS of HPV16 L2 can bind promiscuously to DNA *in vitro* (Klucsevsek et al., 2006), it is not known whether this NRS binds the viral genome *in vivo*. Significantly, analysis of HPV16 infectivity in a murine challenge model and in HaCaT human keratinocytes using pseudovirions with 16L2 mutants containing mutations in the NRS (RR297AA and RR297EE) that inhibit 16L2 nuclear retention, revealed a strong inhibition of infectivity almost to the background level. These data clearly suggest that the nuclear retention of HPV16 L2 mediated by its NRS is critical during the initial phase of HPV16 infection *in vivo*. It would be of great interest to determine in the future the exact step during infection that is affected by a defective L2's NRS. One possibility is that this NRS of 16L2 might be involved in the nuclear retention of the L2-viral genome complex during the initial phase of HPV infection. Mapping studies by Becker et al. (2003) suggest that this NRS is not involved in binding to ND-10, an interaction that potentiates infection and requires PML (Day et al., 2004). It is noteworthy that L2 also interacts with numerous other nuclear proteins defined by yeast 2-hybrid studies and co-localization, including PATZ and PLINP (Gornemann et al., 2002), but their relationship to the NRS and infection remains to be determined.

The results showing that the RJA nuclear export inhibitor causes partial re-localization of 16L2 nuclear retention mutants into the nucleus indicated that 16L2 could also exit the nucleus via a CRM1-dependent export pathway. Indeed, motif analysis followed by mutagenesis-localization investigation revealed that 16L2 contains also a leucine-rich cNES (₄₆₂LPYFFSDVSL₄₇₁), which can mediate nuclear export of 16L2 in a CRM1-dependent manner. The ₄₆₂L and ₄₆₅FF residues were essential for the cNES export function, as their mutagenesis to alanine inhibited nuclear export and as a consequence rescued the nuclear localization of the 16L2 nuclear retention mutants. Significantly, this cNES of 16L2 is well conserved in other L2 proteins of high risk types 31 and 33 and partially conserved in the L2 proteins of low risk HPV types 6 and 11 (Table 3). It will be interesting to determine if the corresponding NES sequences function in nuclear export for other HPV types. A previous study showed that HPV16 pseudovirions containing a C-terminally truncated 16L2 mutant, 1–464, with partially deleted cNES (₄₆₂LPY_) had only 16% infectivity in comparison with the wild type 16L2 after 72 h post-infection in 293TT cells (Florin et al., 2006). Our *in vivo* analysis of HPV16 infection of the murine vaginal tract with pseudoviruses containing L2 NES mutants defective in L2 nuclear export, revealed that both mutations reduced infectivity, although less

Table 1
Effect of mutations in the NRS and NES of HPV16 L2 on reporter DNA encapsidation.

HPV16 L2 status	% DNA packing vs. WT
WT	100
RR297EE	86
RR297AA	35
FF465AA	49
V469_	144

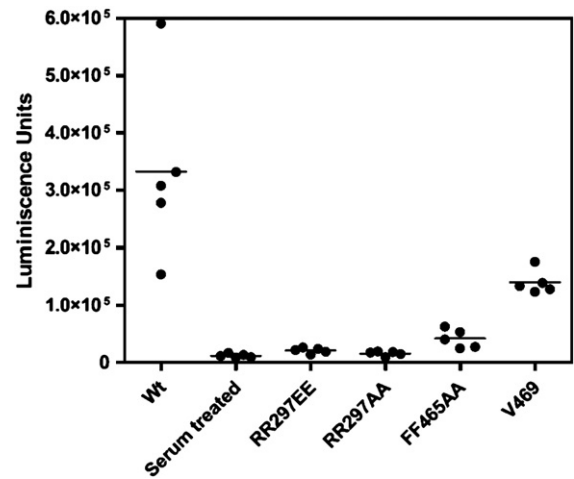


Fig. 8. The effect of mutations in the NRS and NES of 16L2 on HPV infection of the murine vaginal tract. Wild type and L2 mutant pseudoviruses were applied intravaginally in each mouse (5 mice per group) and after 72 h the mice were anesthetized, luciferin was deposited intravaginally and the images were recorded with a Xenogen IVIS 200. The raw data were computed using Living Image software (Caliper Life Sciences) and the bioluminescence data are plotted for each group.

pronounced than the NRS mutations (to 13% of wild type for the FF465AA mutant and to 42% of wild type for the V469_ mutant). There was also some reduction of infectivity with these 2 NES L2 mutants in HaCaT cells, again less pronounced than for the NRS mutants. Between these two L2 NES mutations, the FF465AA mutation had a slightly stronger inhibitory activity on nuclear export and consequently rescued the nuclear localization of the 16L2ms4 NRS mutant to wild type levels at $92 \pm 5.4\%$ (Fig. 6B) in comparison with the V469_ deletion mutation that rescued the nuclear localization to $83.7 \pm 7.5\%$ (Fig. 4B).

The cNES of 16L2 partially overlaps with the dynein-binding domain mapped to the C-terminal 40 amino acids of 16L2 and the dynein–L2 interaction is required for infectivity (Florin et al., 2006). As the dynein-binding domain partially overlaps with the cNES we cannot exclude the possibility that the 16L2 FF465AA mutation may also affect dynein binding. Consequently, the reduction in infectivity with the L2 FF465AA mutant pseudovirus could be due to reduced dynein binding to L2 and to a defective NES.

The discovery that the 16L2 minor capsid protein has a leucine-rich NES that can mediate its nuclear export in a CRM1-dependent

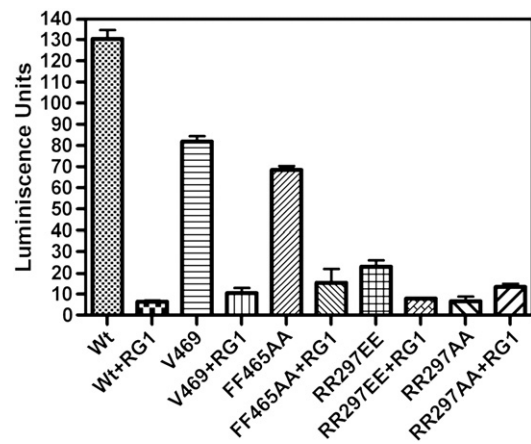


Fig. 9. The effect of mutations in the NRS and NES of 16L2 on HPV infectivity in HaCaT cells. HaCaT cells were incubated for 72 h with equal amounts of HPV16 L2 wild type and mutant pseudoviruses with and without RG1 antibody specific to HPV16 L2. The luciferase activity in cell lysate was determined with a luciferase assay kit and the bioluminescence was measured with a Luminometer.

Table 2

Comparison of the nNLS and cNLS of HPV16 L2 with other L2 proteins of high and low risk HPV types.

HPV type	nNLS	cNLS
HPV16 L2	M R H K R S A K R T K R	R K R R K R
HPV18 L2	M V S H R A A R R K R	K K R K R
HPV33 L2	M R H K R S T R R K R	R R R R K R
HPV11 L2	M K P R A R R R K R	R R R R K R
HPV6b L2	M A H S R A R R R K R	R K R R K R

The basic amino acids K and R characteristic of these NLSs are in bold.

manner raises the question of why the L2 minor capsid protein that has nuclear localization and essential nuclear functions during the viral cycle needs to actively exit the nucleus. One possibility would be that L2 nuclear export could regulate the quantity of L2 in the nucleus allowing only as much L2 as required for genome encapsidation during the productive phase of infection. As L2 also has a membrane-penetrating function and cytotoxic properties via its C-terminus (Kamper et al., 2006), regulating the concentration of L2 in the nucleus would protect the host cell from premature virus-induced nuclear damage, which would be detrimental to viral propagation. Another possibility would be that the interaction of the leucine-rich cNES of 16L2 with CRM1 nuclear export receptor might facilitate the nuclear entry of the viral genome. Future detailed studies would be necessary to determine the step in the viral cycle affected by a defective L2's NES and the potential role of 16L2 nuclear export during HPV infection.

In conclusion, in this study we determined that HPV16 L2 minor capsid protein has several transport signals mediating its nucleocytoplasmic traffic *in vivo*: two NLSs at the N- and C-termini that can independently mediate nuclear import of L2, an arginine-rich NRS in the middle of the protein involved in its nuclear retention and a leucine-rich NES at the C-terminus mediating its nuclear export.

Materials and methods

Generation of EGFP fusion plasmids with HPV16 L2 wild type and mutagenesis

The pEGFPc1 vector (Clontech) was used to express 16L2 in HeLa cells. EGFP-16L2 was constructed as follows: pEGFPc1 was prepared for ligation by double digestion with EcoRI and BamHI at 37 °C for 1 h, and the linearized vector was selectively purified by agarose gel electrophoresis (Qiagen). The HPV16 L2 ORF (1.4 kb) was amplified by the polymerase chain reaction (PCR) with oligonucleotide primers incorporating flanking EcoRI (forward) and BamHI (reverse) cloning sites, in a reaction containing Platinum Pfx DNA Polymerase. The PCR product was purified and then double digested with BamHI and EcoRI for 1 h at 37 °C. The digested vector and PCR product were ligated with T4 DNA ligase (NEB). EGFP-L2ΔN was constructed as EGFP-L2, but with the forward primer omitting the residues 1–12.

Site-directed mutagenesis was performed using the QuikChange™ Site-Directed Mutagenesis Kit from Stratagene with EGFP-16L2 as a

Table 3

Comparison of the NRS and NES of HPV16 L2 with other L2 proteins of high and low risk HPV types.

HPV type	NRS	NES
HPV16 L2	S R R T G I R Y S R I G N K Q T L R T R S	L P Y F F S D V S L
HPV18 L2	S R R G T V R F S R L G Q R A T M F T R S	V P Y F F A D G F V
HPV31 L2	S R R N T V R Y S R L G N K Q T L R T R S	V S Y F F T D V S V
HPV33 L2	S R R H T V R F S R V G Q K A T L K T R S	F P Y F F T D V R V
HPV11 L2	S R R G L V R F S R I G Q R G S M Y T R S	I P L F F S D V A A
HPV6b L2	S R R G L V R Y S R I G Q R G S M H T R S	I P L F F T D V A A

The R and K residues in the NRS and the characteristic hydrophobic residues in the NES are in bold.

template together with corresponding overlapping mutated primers. The deletion mutant EGFP-L2ΔC was generated using deletion primers that omitted residues 456–461 of 16L2 using EGFP-L2 as a template. EGFP-L2ΔNΔC was generated as EGFP-L2ΔC but with EGFP-L2ΔN as a template. The EGFP-16L2ms1(RR297EE), EGFP-16L2ms2(RTR313EEE), EGFP-16L2ms3(RR297EE, RTR313EEE), EGFP-16L2ms4(RR297AA) and EGFP-16L2ms5 (RTR313AAA) plasmids were generated using QuikChange™ Site-Directed Mutagenesis with EGFP-16L2 as a template together with the corresponding overlapping mutated primers in the NRS region. Additional mutations in the potential NESs were generated using EGFP-16L2ms4 as template: 1) in the potential nNES: s1: FF54AA and s2: LGI58AAA, and 2) in the potential cNES: t1: ₄₆₂L_ (containing a stop codon at ₄₆₃P), t2: ₄₆₂LPYFFSD_ (containing a stop codon at ₄₆₉V), and two substitutions, L462A and FF465AA. T1 and t2 deletion mutations of the cNES were also generated using the EGFP-16L2ms5 as template.

All the resulting plasmids were used to transform XL1-Blue cells and the purified plasmids were confirmed by sequencing (Eurofins MWG). After confirmation of mutagenesis, the entire L2 ORF of every mutant was sequenced to confirm the absence of spurious mutations.

Transfections assays and confocal fluorescence microscopy

Transient transfections of HeLa cells (ATCC) with the corresponding EGFP fusion plasmids (as indicated in the figure legends) were performed using the lipid-based FuGENE6 mammalian transfection reagent (Roche). HeLa cells were cultured onto poly-L-lysine (Sigma) coated glass coverslips 24–36 h prior to transfection, at 70–80% confluency in 24-well tissue culture plates. At 24 h post-transfection, cells were washed in cold PBS and fixed for 3 min in 100% methanol at –20 °C. Cells were washed in PBS and either mounted onto glass slides for microscopy using Vectashield mounting medium (Vector Laboratories) with 4,6-diamidinophenylindole (DAPI) to stain the nuclear DNA, or blocked for 1 h in 3% bovine serum albumin (BSA) in PBS and immunostained with RG-1 mouse monoclonal antibody against residues 17–36 of HPV16 L2 (Gambhira et al., 2007) followed by a corresponding secondary antibody conjugated to Alexa Fluor 594. Ratjadone A (RJA), a specific inhibitor of CRM1 nuclear export receptor, was used in drug treatments of transfected cells. At 22 h post-transfection, HeLa cells were treated with 10 ng/mL RJA in DMEM+ for 3.5 h. After treatment, cells were fixed and prepared as above.

Digital images were acquired on a Leica TCS Sp5 confocal microscope. Quantitation of localization was performed when phenotypes were complex, and classified as mostly nuclear, mostly cytoplasmic, or pancellular (both in the nucleus and in the cytoplasm with no specific accumulation). Most quantitations were performed on the RG-1/Alexa 594 immunostaining; some quantitations were performed on the GFP fluorescence. The statistical analysis of the quantitations was presented graphically with average and standard deviation. Immunoblot analysis of whole cell lysates of the transfected cells with EGFP-L2 wild type and different mutants with GFP Ab revealed the presence of the intact EGFP-L2 proteins and also of some free EGFP; the western blots with the RG-1 Ab to L2 detected only the intact EGFP-L2 wild type and the different EGFP-L2 mutants, and as expected did not cross-react with the free EGFP.

Pseudovirus preparation

HPV16 pseudovirions with encapsulated luciferase reporter were generated by cotransfection of 293TT cells with plasmids encoding codon-modified L1 and wild type L2, L2 mutants RR297EE, RR297AA, FF465AA, and V469_, respectively and a firefly luciferase reporter plasmid, as described previously (Pastrana et al., 2004). Cells collected after transfection were matured overnight in Brij 58 (0.5%) and benzonase (0.5%) and pseudovirions were purified by

centrifugation on an OptiPrep step gradient (27, 33, and 39%) at 40,000 rpm for 15 h. The DNA encapsidation for the different pseudoviruses was measured using real-time PCR.

Real-time PCR measurement of encapsidated luciferase reporter DNA

Reporter plasmid DNA containing firefly luciferase was purified from 20 μ l of each HPV pseudovirus samples using PureLink Viral RNA/DNA Kits (Invitrogen). The real-time PCR reactions were conducted using a total volume of 50 μ l, containing 25 μ l of TaqMan Universal PCR Master Mix (Applied Biosystems), 900 nM of forward and reverse primers (TTG ACC GCC TGA AGT CTC TGA and ACA CCT GCG TCG AAG ATG TTG), 250 nM of TaqMan probe (6FAM-CCG CTG AAT TGG AAT CCA TCT TGC TC-TAMRA), and 5 μ l of purified reporter plasmid template using an iCycler IQ (Biorad). Each sample was performed in triplicate. The real-time PCR thermal cycling conditions included AmpliTaq Gold Activation at 95 °C for 10 min, followed by 40 cycles of the PCR step at 95 °C for 15 s and 60 °C for 1 min. FAM fluorescent emission (530 nm wavelength) was measured at the end of the anneal/Extend step. The specificity of each reaction was verified after completion of the protocol by melt curve analysis. The amount of standard template plasmid was from 50 ng to 0.05 μ g.

In vivo pseudovirus delivery and infection

Female Balb/c (6–8 weeks old) were purchased from the National Cancer Institute (Frederick, MD, USA) and kept in the animal facility of the Johns Hopkins School of Medicine (Baltimore, MD, USA). Mouse experiments were approved by the Johns Hopkins University Animal Care and Use Committee. All animal procedures were performed according to approved protocols and in accordance with the recommendations for the proper use and care of laboratory animals. The mice received 3 mg of Depo-provera (Pfizer) 4 days prior to infection as described (Roberts et al., 2007). Animals were infected under anesthesia with a 25 μ g PsV inoculum of 20 μ l mixed with 20 μ l of a 3% CMC preparation. The inoculum was delivered in two doses, 20 μ l before and 20 μ l after Cytobrush treatment, using an M20 positive-displacement pipette. Mice underwent a procedure in conjunction with pseudovirus inoculation in which a Cytobrush cell collector was inserted in the vagina and twirled clockwise and counterclockwise 10 times. The material was delivered with an M20 positive-displacement pipette (Gilson), and standard dissecting forceps were used to occlude the vaginal introitus to achieve maximal retention of the material. For those mice receiving the passively transferred L1 anti-serum, serum (30 μ l) was diluted in 1 \times PBS to a final volume of 100 μ l and was administered intraperitoneally 24 h prior to infection. Infection was measured 72 h after pseudovirus delivery as previously described (Roberts et al., 2007). The raw data were computed using Living Image software (Caliper Life Sciences). An identical region of interest (ROI) was drawn around the luciferase signal emitted from each mouse, and the average radiance within the ROI was determined.

HPV infectivity assays in HaCaT cells

HPV16 pseudovirus infectivity and neutralization assays were carried out as outlined previously (Jagu et al., 2009) in HaCaT cells (a spontaneously immortalized human keratinocyte line). Briefly, HaCaT cells were seeded at 15,000 cells/well in 96-wells plate 24 h prior to the assay. The wild type and mutant pseudoviruses were normalized by L1 protein concentration and $\sim 2.87 \times 10^4$ particles were incubated with HaCaT cells for 72 h with and without RG1 antibody specific to HPV16 L2 at 0.72 μ g concentration. The luciferase activity in the cell lysate was determined with a luciferase assay kit (Promega, Madison, WI) according to the manufacturer's instructions. The

bioluminescence was measured with a Luminometer (Promega Glomax Multidetector system, Promega, Madison, WI, USA).

Supplementary materials related to this article can be found online at doi:10.1016/j.virol.2011.11.007.

Acknowledgments

We thank Kathy Bockstall for initial transfection assays with EGFP-16L2 and Δ N, Δ C and Δ N Δ C mutants. We thank Courtney Halista for technical assistance with plasmid purifications and initial transfections and localization studies for EGFP-16L2ms5 and EGFP-16L2ms5t1. We also thank Dr. Joshua Rosenberg for excellent technical assistance with confocal fluorescence microscopy. This work was supported by a grant from the National Institutes of Health (R01 CA94898) to Junona Moroianu and CA133749, CA118790 and P50 CA098252 and RC2 CA148499 to RBSR.

References

- Becker, K.A., Florin, L., Sapp, C., Sapp, M., 2003. Dissection of human papillomavirus type 33 L2 domains involved in nuclear domains (ND) 10 homing and reorganization. *Virology* 314 (1), 161–167.
- Bordeaux, J., Forte, S., Harding, E., Darshan, M.S., Klucsevsek, K., Moroianu, J., 2006. The L2 minor capsid protein of low-risk human papillomavirus type 11 interacts with host nuclear import receptors and viral DNA. *J. Virol.* 80 (16), 8259–8262.
- Buck, C.B., Cheng, N., Thompson, C.D., Lowy, D.R., Steven, A.C., Schiller, J.T., Trus, B.L., 2008. Arrangement of L2 within the papillomavirus capsid. *J. Virol.* 82 (11), 5190–5197.
- Darshan, M.S., Lucchi, J., Harding, E., Moroianu, J., 2004. The L2 minor capsid protein of human papillomavirus type 16 interacts with a network of nuclear import receptors. *J. Virol.* 78 (22), 12179–12188.
- Day, P.M., Lowy, D.R., Schiller, J.T., 2003. Papillomaviruses infect cells via a clathrin-dependent pathway. *Virology* 307 (1), 1–11.
- Day, P.M., Baker, C.C., Lowy, D.R., Schiller, J.T., 2004. Establishment of papillomavirus infection is enhanced by promyelocytic leukemia protein (PML) expression. *Proc. Natl. Acad. Sci. U.S.A.* 101 (39), 14252–14257.
- Fay, A., Yutzy, W.H.T., Roden, R.B., Moroianu, J., 2004. The positively charged termini of L2 minor capsid protein required for bovine papillomavirus infection function separately in nuclear import and DNA binding. *J. Virol.* 78 (24), 13447–13454.
- Florin, L., Sapp, C., Streeck, R.E., Sapp, M., 2002. Assembly and translocation of papillomavirus capsid proteins. *J. Virol.* 76 (19), 10009–10014.
- Florin, L., Becker, K.A., Lambert, C., Nowak, T., Sapp, C., Strand, D., Streeck, R.E., Sapp, M., 2006. Identification of a dynein interacting domain in the papillomavirus minor capsid protein L2. *J. Virol.* 80 (13), 6691–6696.
- Gambhira, R., Karanam, B., Jagu, S., Roberts, J.N., Buck, C.B., Bossis, I., Alphas, H., Culp, T., Christensen, N.D., Roden, R.B., 2007. A protective and broadly cross-neutralizing epitope of human papillomavirus L2. *J. Virol.* 81 (24), 13927–13931.
- Gornemann, J., Hofmann, T.G., Will, H., Muller, M., 2002. Interaction of human papillomavirus type 16 L2 with cellular proteins: identification of novel nuclear body-associated proteins. *Virology* 303 (1), 69–78.
- Holmgren, S.C., Patterson, N.A., Ozbun, M.A., Lambert, P.F., 2005. The minor capsid protein L2 contributes to two steps in the human papillomavirus type 31 life cycle. *J. Virol.* 79 (7), 3938–3948.
- Hutten, S., Kehlenbach, R.H., 2007. CRM1-mediated nuclear export: to the pore and beyond. *Trends Cell Biol.* 17 (4), 193–201.
- Jagu, S., Karanam, B., Gambhira, R., Chivukula, S.V., Chaganti, R.J., Lowy, D.R., Schiller, J., Roden, R.B.S., 2009. Concatenated multitype L2 fusion proteins as candidate prophylactic pan-human papillomavirus vaccines. *JNCI* 101 (11), 782–792.
- Kamper, N., Day, P.M., Nowak, T., Selinka, H.C., Florin, L., Bolscher, J., Hilbig, L., Schiller, J.T., Sapp, M., 2006. A membrane-destabilizing peptide in capsid protein L2 is required for egress of papillomavirus genomes from endosomes. *J. Virol.* 80 (2), 759–768.
- Karanam, B., Peng, S., Li, T., Buck, C., Day, P.M., Roden, R.B., 2010. Papillomavirus infection requires gamma secretase. *J. Virol.* 84 (20), 10661–10670.
- Klucsevsek, K., Daley, J., Darshan, M.S., Bordeaux, J., Moroianu, J., 2006. Nuclear import strategies of high-risk HPV18 L2 minor capsid protein. *Virology* 352 (1), 200–208.
- Lanosz, V., Nguyen, K.C., Meneses, P.I., 2007. Bovine papillomavirus type 1 infection is mediated by SNARE syntaxin 18. *J. Virol.* 81 (14), 7435–7448.
- Lin, Z., Yemelyanova, A.V., Gambhira, R., Jagu, S., Meyers, C., Kirnbauer, R., Ronnett, B.M., Gravitt, P.E., Roden, R.B., 2009. Expression pattern and subcellular localization of human papillomavirus minor capsid protein L2. *Am. J. Pathol.* 174 (1), 136–143.
- Longworth, M.S., Laimins, L.A., 2004. Pathogenesis of human papillomaviruses in differentiating epithelia. *Microbiol. Mol. Biol. Rev.* 68 (2), 362–372.
- Meissner, T., Krause, E., Vinkemeier, U., 2004. Ratjadone and leptomycin B block CRM1-dependent nuclear export by identical mechanisms. *FEBS Lett.* 576 (1–2), 27–30.
- Pastrana, D.V., Buck, C.B., Pang, Y.Y., Thompson, C.D., Castle, P.E., FitzGerald, P.C., Kruger Kjaer, S., Lowy, D.R., Schiller, J.T., 2004. Reactivity of human sera in a sensitive, high-throughput pseudovirus-based papillomavirus neutralization assay for HPV16 and HPV18. *Virology* 321 (2), 205–216.

- Richards, R.M., Lowy, D.R., Schiller, J.T., Day, P.M., 2006. Cleavage of the papillomavirus minor capsid protein, L2, at a furin consensus site is necessary for infection. *Proc. Natl. Acad. Sci. U.S.A.* 103 (5), 1522–1527.
- Roberts, J.N., Buck, C.B., Thompson, C.D., Kines, R., Bernardo, M., Choyke, P.L., Lowy, D.R., Schiller, J.T., 2007. Genital transmission of HPV in a mouse model is potentiated by nonoxynol-9 and inhibited by carrageenan. *Nat. Med.* 13 (7), 857–861.
- Roden, R.B., Day, P.M., Bronzo, B.K., Yutzy, W.H.t., Yang, Y., Lowy, D.R., Schiller, J.T., 2001. Positively charged termini of the L2 minor capsid protein are necessary for papillomavirus infection. *J. Virol.* 75 (21), 10493–10497.
- Sapp, M., Bienkowska-Haba, M., 2009. Viral entry mechanisms: human papillomavirus and a long journey from extracellular matrix to the nucleus. *FEBS J.* 276 (24), 7206–7216.
- Smith, J.L., Campos, S.K., Ozbun, M.A., 2007. Human papillomavirus type 31 uses a caveolin 1- and dynamin 2-mediated entry pathway for infection of human keratinocytes. *J. Virol.* 81 (18), 9922–9931.
- Smith, J.L., Campos, S.K., Wandler-Ness, A., Ozbun, M.A., 2008. Caveolin-1-dependent infectious entry of human papillomavirus type 31 in human keratinocytes proceeds to the endosomal pathway for pH-dependent uncoating. *J. Virol.* 82 (19), 9505–9512.
- Spoden, G., Freitag, K., Husmann, M., Boller, K., Sapp, M., Lambert, C., Florin, L., 2008. Clathrin- and caveolin-independent entry of human papillomavirus type 16—involvement of tetraspanin-enriched microdomains (TEMs). *PLoS One* 3 (10), e3313.
- Sun, X.Y., Frazer, I., Muller, M., Gissmann, L., Zhou, J., 1995. Sequences required for the nuclear targeting and accumulation of human papillomavirus type 6B L2 protein. *Virology* 213 (2), 321–327.
- Yang, R., Yutzy, W.H.t., Viscidi, R.P., Roden, R.B., 2003. Interaction of L2 with beta-actin directs intracellular transport of papillomavirus and infection. *J. Biol. Chem.* 278 (14), 12546–12553.
- zur Hausen, H., 2009. Papillomaviruses in the causation of human cancers—a brief historical account. *Virology* 384 (2), 260–265.